European Journal of Medicinal Chemistry 76 (2014) 549–557

Contents lists available at ScienceDirect

European Journal of Medicinal Chemistry

journal homepage: http://www.elsevier.com/locate/ejmech

Original article

Design, synthesis and molecular modeling of pyrazole–quinoline–pyridine hybrids as a new class of antimicrobial and anticancer agents

Chetan B. Sangani, Jigar A. Makawana, Xin Zhang, Shashikant B. Teraiya, Lin Lin, Hai-Liang Zhu*

State Key Laboratory of Pharmaceutical Biotechnology, Nanjing University, Nanjing 210093, China

ARTICLE INFO

Article history:
Received 3 December 2013
Received in revised form
7 January 2014
Accepted 13 January 2014
Available online 25 January 2014

Keywords:
4*H*-Quinoline
1*H*-Pyrazole-4-carbaldehyde
Pyridine
One-pot reaction
Antibacterial activity
Anticancer activity
Molecular modeling

ABSTRACT

A new series of pyrazole–quinoline–pyridine hybrids were designed based on molecular hybridization technique and synthesized by a base-catalyzed cyclocondensation reaction through one-pot multicomponent reaction. All compounds were tested for *in vitro* antibacterial and anticancer activities. Enzyme inhibitory activities of all compounds were carried out against FabH and EGFR. Of the compounds studied, majority of the compounds showed effective antibacterial as well as anticancer activity against used strains and cancer cell lines respectively. Compound **7k** ($IC_{50} = 0.51 \pm 0.05$ μM) against EGFR and **7b** displayed the most potent inhibitory activity with IC_{50} of 3.1 μM against FabH as compared to other member of the series. In the molecular modeling study, compound **7k** was bound in to the active pocket of EGFR with three hydrogen bond and one π–cation interaction with minimum binding energy $\Delta G_b = -54.6913$ kcal/mol, as well as compound **7b** was bound in to the active site of FabH with hydrogen bond and π–sigma interactions with minimum binding energy $\Delta G_b = -45.9125$ kcal/mol.

1. Introduction

Along with the living habits and environment changes, cancer has become the major cause of death in both developing and developed countries [1]. Until now one significant way to induce the occurrence of cancers is still by mutation or mis-regulation of cell cycle regulatory genes and proteins to guide an abnormal control of cell proliferation [2]. Epidermal growth factor receptor (EGFR) is a kind of tyrosine kinase firstly reported in the literature [3,4]. It has become one of the targets of anticancer drug research and development because of it's widely distribution in the cell and important role in cell life. EGFRs are distributed in mammalian epithelial cell membranes and have relationships with cell proliferation, death, and differentiation. They are junctions to deliver extracellular growth signals intracellular. EGFR family comprise four members, including: EGFR (HER1/ErbB-1), ErbB-2 (HER2/neu), ErbB-3 (HER3), and ErbB-4 (HER4) [5]. EGFR tyrosine kinase-mediated cell growth signaling pathway plays an important role in the formation and development of many types of solid tumors, such as nonsmall cell lung cancer [6], head and neck cancer [7] and glioblastomas [8]. Overexpression of EGFR family receptors have always been observed in these tumors, approximately in 60% of all tumors [6]. EGFR and ErbB-2 are the hottest targets in current research and their over expression or abnormal activation often cause cell malignant transformation. Also they have relationship with postoperative adverse, radiotherapy and chemotherapy resistance and tumor angiogenesis [9].

Besides, bacteria resistant to known therapies are a growing threat across the globe. An increasing fraction of bacterial isolates shows reduced susceptibility to our most trusted antibiotics. In order to prevent this serious medical problem, the discovery of new types of antibacterial agents or the expansion of bioactivity of the previous drugs is a very important task [10]. Therefore, in recent years, the research has been focused on the development of new antibacterial agents, which may act through structure design and novel targets, overcoming the problem of acquired resistance. One of the most attractive biochemical pathways that could be targeted for new antibacterial agents is the fatty acid biosynthesis (FAS). This pathway has been demonstrated to be essential for the bacteria cell survival [11] and differs considerably from human FAS pathway. While in humans fatty acid synthesis occurs in a homodimeric multifunctional enzyme [12,13] in bacteria the pathway is composed of various discrete enzymes and each one can be considered a putative molecular target. Those features make the type II FAS pathway a potential target for new antimicrobial agents.

* Corresponding author. Tel.: +86 25 83592572.
E-mail address: zhuhl@nju.edu.cn (H.-L. Zhu).

0223-5234/$ – see front matter © 2014 Elsevier Masson SAS. All rights reserved.
http://dx.doi.org/10.1016/j.ejmech.2014.01.018

A key enzyme in this pathway is the β-ketoacyacyl carrier protein synthase III (FabH), which is the responsible enzyme of the first pathway reaction and play an important regulatory role. FabH has also been demonstrated to be essential for organism survival and it is presented in a wide number of important human pathogens. Furthermore, some chemical compounds have shown to inhibit FabH from diverse microl-organisms, including multi-drug resistant strains [14,15] These facts support the idea that FabH can be used as an effective molecular target for the development of new antimicrobial agents. Over the past few years, we have been principally engrossed in the synthesis of pyrazole incorporating structures for biological evaluations [16–21] on the premise that the several 4-functionally substituted *N*-arylpyrazole derivatives identified as antimicrobial [22–24], anti-inflammatory (COX-2 inhibitor and ulcerogenic activity) [23], antitubercular [24], antitumor [25,26], anticancer [27–30] as well as inhibitory activity against FabH [31]. Furthermore, quinoline moiety is found in a large variety of naturally occurring compounds and also chemically useful synthons bearing diverse bioactivities [32–42] including EGFR inhibitory activity [43]. Also, no one can ignore the role of pyridine as an appreciable pharmacophore for antimicrobial and anticancer activity [44,45] including EGFR inhibitory activity [46]. Moreover, multicomponent reactions were employed as a powerful tool to synthesize diverse and complex heterocyclic compounds due to their advantages of the intrinsic atom economy, simpler procedures, structural diversity, energy savings, and reduced waste [47–49]. In view of biological significance of pyrazole, quinoline and pyridine a modification on the 1 and 4-position on 4*H*-quinoline by pyridine and 1*H*-pyrazole-4-carbaldehydes respectively may bring significant changes in pharmacological activities and may provide new classes of therapeutically active compounds, with this hope and as a part of our current studies in developing new therapeutically active agents *via* combination of two therapeutically active moieties [16–21], we report herein the preparation of *N*-pyridinyl-4-pyrazolyl-4*H*-quinoline **7a–l** derivatives *via* MCR approach i.e. one pot base-catalyzed cyclocondensation reaction of 1*H*-pyrazole-4-carbaldehydes, malononitrile/ethylcyanoacetate and β-pyridinyle naminone.

2. Chemistry

The synthetic approach adopted to obtain the target compounds is depicted in Scheme 1. The starting material 1-aryl-5-chloro-3-methyl-1*H*-pyrazole-4-carbaldehydes **2a–c** was prepared according to literature procedure [16] by Vilsmeier–Haack reaction of 1-aryl-3-methyl-1*H*-pyrazol-5(4*H*)-one **1a–c**. The required 3-(pyridin-3-*yl*amino)cyclohex-2-enones **5a**, **b** were synthesized by nucleophilic addition reaction of 1,3-cyclohexanedione/dimedone **3a**, **b** and 3-aminopyridine **4** at 120 °C for 30 min under solvent free condition [32]. The title compounds **7a–l** were prepared *via* one-pot three component cyclocondensation reaction between **2a–c**, **5a**, **b** and malononitrile/ethylcyanoacetate **6a**, **b** in ethanol containing a catalytic amount of piperidine in good to excellent yields.

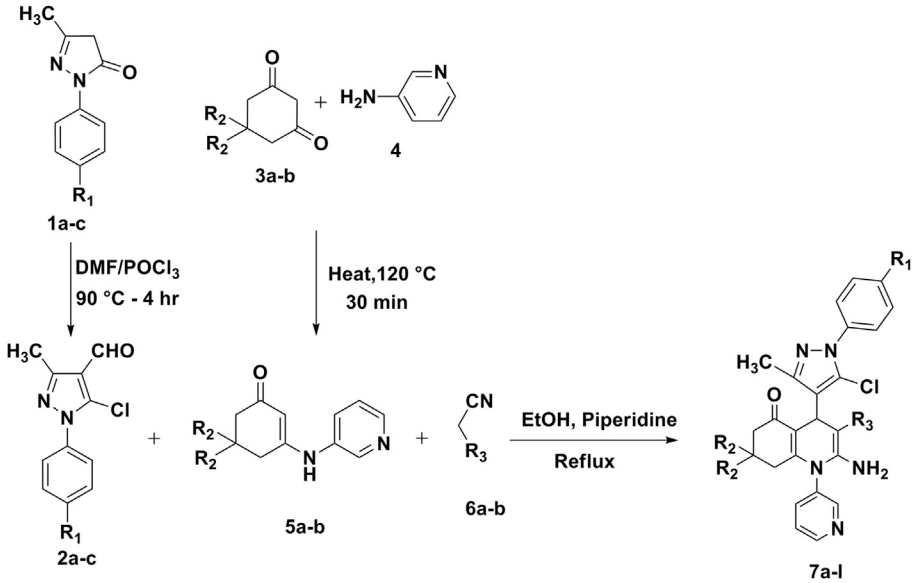

Comp	R_1	R_2	R_3	Comp	R_1	R_2	R_3
7a	H	H	CN	**7g**	H	H	COOEt
7b	CH_3	H	CN	**7h**	CH_3	H	COOEt
7c	Cl	H	CN	**7i**	Cl	H	COOEt
7d	H	CH_3	CN	**7j**	H	CH_3	COOEt
7e	CH_3	CH_3	CN	**7k**	CH_3	CH_3	COOEt
7f	Cl	CH_3	CN	**7l**	Cl	CH_3	COOEt

Scheme 1. Synthetic pathway for the synthesis of title derivatives **7a–l**.

The reaction occurs *via* an *in situ* initial formation of the heterylidenenitrile, containing the electron-poor C=C double bond, from the Knoevenagel condensation between pyrazole-4-carbaldehyde and malononitrile/ethylcyanoacetate by loss of water molecules. Finally, Michael addition of **5a**, **b** to the initially formed unsaturated nitrile, i.e. nucleophilic attack of enaminone to the cyano moiety affords cyclized 4*H*-quinoline derivatives **7a**–**l** (Scheme 2).

3. Biological assay

3.1. Experimental method for cell proliferation assay

The antiproliferative activities of 4*H*-quinoline derivatives **7a**–**l** were determined using a standard (MTT)-based colorimetric assay (Sigma). Briefly, cell lines were seeded at a density of 7×10^3 cells/well in 96-well microtiter plates (Costar). After 24 h, exponentially growing cells were exposed to the indicated compounds at final concentrations ranging from 0.1 to 40 mg/mL. After 48 h, cell survival was determined by the addition of an MTT solution (20 μL of 5 mg/mL MTT in PBS). After 6 h, 100 mL of 10% SDS in 0.01 N HCl was added, and the plates were incubated at 37 °C for a further 4 h; optical absorbance was measured at 570 nm on an LX300 Epson Diagnostic microplate reader. Survival ratios are expressed in percentages with respect to untreated cells. IC_{50} values were determined from replicates of 6 wells from at least two independent experiments.

3.2. General procedure for preparation, purification of EGFR inhibitory assay

A 1.6 kb cDNA encoded for the EGFR cytoplasmic domain (EGFR-CD, amino acids 645-1186) were cloned into baculoviral expression vectors pBlueBacHis2B and pFASTBacHTc (Huakang Company China), separately. A sequence that encodes $(His)_6$ was located at the 50 upstream to the EGFR sequences. Sf-9 cells were infected for 3 days for protein expression. Sf-9 cell pellets were solubilized at 0 °C in a buffer at pH 7.4 containing 50 mM HEPES, 10 mM NaCl, 1% Triton, 10 μM ammonium molybdate, 100 μM sodium vanadate, 10 μg/mL aprotinin, 10 μg/mL leupeptin, 10 μg/mL pepstatin, and 16 μg/mL benzamidine HCl for 20 min followed by 20 min centrifugation. Crude extract supernatant was passed through an equilibrated Ni-NTA superflow packed column and washed with 10 mM and then 100 mM imidazole to remove nonspecifically bound material. Histidinetagged proteins were eluted with 250 and 500 mM imidazole and dialyzed against 50 mM NaCl, 20 mM HEPES, 10% glycerol, and 1 μg/mL each of aprotinin, leupeptin, and pepstatin for 2 h. The entire purification procedure was performed at 4 °C or on ice [50].

The EGFR kinase assay was set up to assess the level of autophosphorylation based on DELFIA/Time-Resolved Fluorometry. Compounds **7a**–**l** was dissolved in 100% DMSO and diluted to the appropriate concentrations with 25 mM HEPES at pH 7.4. In each well, 10 μL compound was incubated with 10 μL (5 ng for EGFR) recombinant enzyme (1:80 dilution in 100 mM HEPES) for 10 min at room temperature. Then, 10 μL of 5× buffer (containing 20 mM HEPES, 2 mM $MnCl_2$, 100 μM Na_3VO_4, and 1 mM DTT) and 20 μL of 0.1 mM ATP–50 mM $MgCl_2$ were added for 1 h. Positive and negative controls were included in each plate by incubation of enzyme with or without ATP–$MgCl_2$. At the end of incubation, liquid was aspirated, and plates were washed three times with wash buffer. A 75 μL (400 ng) sample of europiumlabeled antiphosphotyrosine antibody was added to each well for another 1 h of incubation. After washing, enhancement solution was added and the signal was detected by Victor (Wallac Inc.) with excitation at 340 nm and emission at 615 nm. The percentage of autophosphorylation inhibition by the compounds was calculated using the following equation: 100% – [(negative control)/(positive control – negative control)]. The IC_{50} was obtained from curves of percentage inhibition with eight concentrations of compound. As

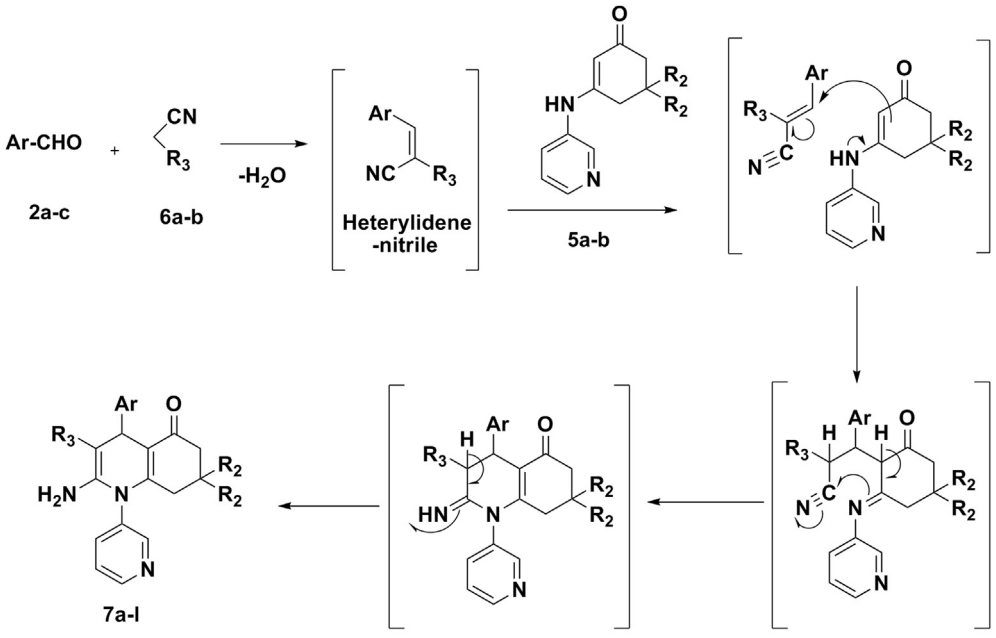

Scheme 2. Plausible mechanistic pathway for title derivatives **7a**–**l**.

the contaminants in the enzyme preparation are fairly low, the majority of the signal detected by the anti-phosphotyrosine antibody is from EGFR.

3.3. Experimental method for antibacterial activity

The antibacterial activity of the synthesized compounds **7a–l** was tested against *Bacillus subtilis*, *Staphylococcus aureus*, *Escherichia coli* and *Pseudomonas aeruginosa* and using MH medium (Mueller–Hinton medium: casein hydrolyzate 17.5 g, soluble starch 1.5 g, beef extract 1000 mL). The MICs (minimum inhibitory concentrations) of the test compounds were determined by a colorimetric method using the dye MTT (3-(4,5-dimethylthiazol-2-yl)-2,5-diphenyl tetrazoliumbromide) [51]. A stock solution of the synthesized compound (100 μg/mL) in DMSO was prepared and graded quantities of the test compounds were incorporated in specified quantity of sterilized liquid MH medium. A specified quantity of the medium containing the compound was poured into microtitration plates. Suspension of the microorganism was prepared to contain approximately 10^5 cfu/mL and applied to microtitration plates with serially diluted compounds in DMSO to be tested and incubated at 37 °C for 24 h. After the MICs were visually determined on each of the microtitration plates, 50 μL of PBS (phosphate buffered saline 0.01 mol/L, pH 7.4, $Na_2HPO_4{\cdot}12H_2O$ 2.9 g, KH_2PO_4 0.2 g, NaCl 8.0 g, KCl 0.2 g, distilled water 1000 mL) containing 2 mg of MTT/mL was added to each well. Incubation was continued at room temperature for 4–5 h. The content of each well was removed, and 100 μL of isopropanol containing 5% 1 mol/L HCl was added to extract the dye. After 12 h of incubation at room temperature, the optical density (OD) was measured with a microplate reader at 550 nm. The observed MICs are presented in Table 2.

3.4. E. coli FabH purification and activity assay

Full-length *E. coli* acyl carrier protein (ACP), acyl carrier protein synthase (ACPS) and b-ketoacyl-ACP synthase III (FabH) were individually cloned into pET expression vectors with an N-terminal His-tag (ACP, ACPS in pET19; FabH in pET28).

All proteins were expressed in *E. coli* strain BL21(DE3). Transformed cells were grown on Luria–Bertani (LB) agar plates supplemented with kanamycin (30 mg/mL). Sodium dodecyl sulfate–polyacrylamide gel electrophoresis (SDS–PAGE) analysis was used to screen colonies for overexpression of proteins. One such positive colony was used to inoculate 10 mL of LB medium with 30 mg/mL of kanamycin and grown over night at 37 °C, 1 mL of which was used to inoculate 100 mL LB medium supplemented with 30 μg/mL of kanamycin. The culture was shaken for 4 h at 37 °C, and then induced with 0.5 mM isopropyl β-D-thiogalactopyranoside (IPTG). The culture was grown for 4 h, and harvested by centrifugation (30 min at 15,000 rpm).

Harvested cells containing His-tagged ACP, ACPS and FabHs were lysed by sonication in 20 mM Tris, pH 7.6, 5 mM imidazole, 0.5 M NaCl and centrifuged at 20,000 rpm for 30 min. The supernatant was applied to a Ni-NTA agarose column, washed and eluted using a 5–500 mM imidazole gradient over 20 column volumes. Eluted protein was dialyzed against 20 mM Tris, pH 7.6, 1 mM DTT and 100 mM NaCl. Purified FabHs were concentrated up to 2 mg/mL and stored at −80 °C in 20 mM Tris, pH 7.6, 100 mM NaCl, 1 mM DTT and 20% glycerol for enzymatic assays. Purified ACP contains the apo-form that needs to be converted into the holo-form. The conversion reaction is catalyzed by ACP synthase (ACPS). In the final volume of 50 mL, 50 mg ACP, 50 mM Tris, 2 mM DTT, 10 mM $MgCl_2$, 600 μM CoA and 0.2 μM ACPS was incubated for 1 h at 37 °C. The pH of the reaction was then adjusted to approximately 7.0 using 1 M potassium phosphate. Holo-ACP was purified by fractionation of the reaction mixture by Source Q-15 ion exchange chromatography using a 0–500 mM NaCl gradient over 2 column volumes.

In a final 20 μL reaction, 20 mM Na_2HPO_4/NaH_2PO_4, pH 7.0, 0.5 mM DTT, 0.25 mM $MgCl_2$ and 2.5 mM holo-ACP were mixed with 1 nM FabH, and H_2O was added to 15 μL. After 1 min incubation, a 2 μL mixture of 25 μM acetyl-CoA and 0.75 μCi [^{3}H] acetyl-CoA was added for FabH reaction for 25 min. The reaction was stopped by adding 20 μL of ice-cold 50% TCA, incubating for 5 min on ice, and centrifuging to pellet the protein. The pellet was washed with 10% ice-cold TCA and resuspended with 5 μL of 0.5 M NaOH. The incorporation of the ^{3}H signal in the final product was read by liquid scintillation. When determining the inhibition constant (IC_{50}), inhibitors were added from a concentrated DMSO stock such that the final concentration of DMSO did not exceed 2%.

3.5. Docking simulations

Molecular docking of all compounds into the three-dimensional EGFR complexstructure (PDB code: 1M17) http://www.rcsb.org/pdb/explore/explore.do?structureId=1M17 as well as into the three-dimensional X-ray structure of *E. coli* FabH (PDB code: 1HNJ) http://www.rcsb.org/pdb/explore/explore.do?structureId=1HNJ were carried out using the AutoDock software package (version 4.0) as implemented through the graphical user interface AutoDock Tool Kit (ADT 1.4.6) [52].

Table 1
Inhibition of EGFR kinase and antiproliferative activity IC_{50} (μM) of compounds **7a–l**.

Compound	EGFR	A549	Hep G2
7a	18.02 ± 0.12	21.05 ± 0.01	10.20 ± 0.02
7b	10.12 ± 0.05	15.10 ± 0.06	29.18 ± 0.11
7c	4.15 ± 0.30	2.15 ± 0.03	9.13 ± 0.06
7d	32.13 ± 0.42	12.18 ± 0.19	15.17 ± 0.21
7e	14.70 ± 0.09	10.67 ± 0.04	4.83 ± 0.15
7f	24.05 ± 0.10	19.10 ± 0.05	1.02 ± 0.08
7g	2.09 ± 0.05	3.18 ± 0.01	7.15 ± 0.03
7h	0.91 ± 0.02	0.25 ± 0.13	1.30 ± 0.05
7i	6.15 ± 0.07	2.10 ± 0.09	5.84 ± 0.12
7j	11.18 ± 0.10	20.08 ± 0.19	24.40 ± 0.04
7k	0.51 ± 0.05	0.18 ± 0.09	4.04 ± 0.05
7l	1.03 ± 0.02	0.21 ± 0.16	6.21 ± 0.16
Erlotinib	0.032 ± 0.002	0.13 ± 0.01	0.12

Table 2
Antibacterial activity of compounds **7a–l**.

Compounds	Minimum inhibitory concentrations (μg/mL)			
	Gram positive		Gram negative	
	B. subtilis ATCC6633	*S. aureus* ATCC6538	*E. coli* ATCC35218	*P. aeruginosa* ATCC13525
7a	6.25	50	25	50
7b	3.13	6.25	1.56	50
7c	12.5	25	50	12.5
7d	50	25	25	50
7e	25	25	25	6.25
7f	25	12.5	6.25	25
7g	12.5	>50	50	25
7h	6.25	50	50	6.25
7i	6.25	3.13	3.13	>50
7j	3.13	12.5	25	12.5
7k	12.5	>50	6.25	>50
7l	>50	50	6.25	25
Kanamycin B	0.39	1.56	1.56	3.13
Penicillin G	1.56	6.25	3.13	6.25

4. Results and discussion

4.1. Analytical results

The structural elucidation of the synthesized compounds **7a**–**l** was carried out by FT-IR, ^{1}H NMR, ^{13}C NMR, elemental analysis and mass spectrometry. In FT-IR spectra, compounds **7a**–**l** exhibited an absorption band around 1635–1645 and 1660–1680 cm^{-1} for (C=O) stretching and 765–740 cm^{-1} for C–Cl group. The characteristic absorption bands for all the compounds were observed in the range of 3445–3350 and 3190–3150 cm^{-1} corresponding to asymmetrical and symmetrical stretching of NH_2 group and 2205–2185 cm^{-1} for C≡N group. In ^{1}H NMR spectra of compounds **7a**–**l**, a sharp singlet peak of methine proton (H_4) was appeared around δ 5.12–5.38 ppm. A most characteristic positive signal observed around δ 34.58–35.28 ppm was indicated methane carbon (C_4) in ^{13}C NMR spectra of compounds **7a**–**l** which confirm the formation of quinoline ring. Also the signal at around δ 59.52–59.64 ppm is assigned to carbon attached with carbonitrile and δ 77.95–78.05 ppm is assigned to carbon attached with ester group. In ^{13}C NMR spectra, the negative signals around δ 169.32–169.48 and 194.87–195.62 were arise for the carbonyl carbon (C=O) of ester and cyclohexenone ring, respectively. The obtained elemental analysis values are in consonance with theoretical data. Mass spectra of title compounds showed expected molecular ion peak M^+ corresponding with proposed molecular mass.

4.2. Biological evaluation

4.2.1. Antiproliferation and EGFR inhibitory activity

All compounds were tested against EGFR kinase as well as against cancer cell A549 (adenocarcinomic human alveolar basal epithelial cell line) and Hep G2 (liver cancer cell line). Upon investigation of antiproliferative activity of compounds **7a**–**l**, it has been observed that compounds **7h** (IC_{50} = 0.25 ± 0.13 μM), **7k** (IC_{50} = 0.18 ± 0.09 μM) and **7l** (IC_{50} = 0.21 ± 0.16 μM) against A549 as well as compounds **7f** (IC_{50} = 1.02 ± 0.08 μM) and **7h** (IC_{50} = 1.30 ± 0.05 μM) against Hep G2 showed most effective activity as compared to other compounds.

As shown in Table 1, compounds **7h** (IC_{50} = 0.91 ± 0.02 μM), **7k** (IC_{50} = 0.51 ± 0.05 μM) and **7l** (IC_{50} = 1.03 ± 0.02 μM) displayed the most potent inhibitory activity against EGFR as compared to other compounds and less comparable to the positive control erlotinib (IC_{50} = 0.032 ± 0.02 μM).

4.2.2. Antibacterial and E. coli FabH inhibitory activity

Upon investigation of antibacterial activity (Table 2), it has been observed that majority of the compounds have shown effective activity against used strains. Against Gram negative bacteria *E. coli*, compound **7b** (MIC = 1.56 μg/mL) showed most effective activity which is more effective than penicillin G (MIC = 3.13 μg/mL) and comparable to kanamycin B (MIC = 1.56 μg/mL), while compound **7i** (MIC = 3.13 μg/mL) showed comparable activity to penicillin G (MIC = 3.13 μg/mL). Compounds **7e** (MIC = 6.25 μg/mL) and **7h** (MIC = 6.25 μg/mL) showed comparable activity to penicillin G (MIC = 6.25 μg/mL) against Gram negative bacteria *P. aeruginosa*. Against Gram positive bacterial *S. aureus*, compounds **7i** (MIC = 3.13 μg/mL) showed more effective activity and **7b** (MIC = 6.25 μg/mL) showed comparable activity as compared to penicillin G (MIC = 6.25 μg/mL). Compounds **7b** (MIC = 3.13 μg/mL) and **7j** (MIC = 3.13 μg/mL) showed effective activity as compared to other compounds against *B. subtilis*.

The *E. coli* FabH inhibitory potency of the synthetic **7a**–**l** derivatives was examined and the results are summarized in Table 3.

Table 3
E. coli FabH inhibitory activity of synthetic compounds **7a**–**l**.

Compounds	*E. coli* FabH IC_{50} (μM)	Hemolysis LC30[a] (mg/ml)
7a	31.8	>10
7b	3.1	>10
7c	12.7	>10
7d	22.1	>10
7e	10.8	>10
7f	5.6	>10
7g	10.1	>10
7h	8.3	>10
7i	6.8	>10
7j	4.5	>10
7k	5.7	>10
7l	9.8	>10

[a] Lytic concentration 30%.

Most of the tested compounds showed potent *E. coli* FabH inhibitory activity. Among them, compound **7b** showed the most potent inhibitory with IC_{50} of 3.1 μM. This result supported the potent antibacterial activity of **7b**. Among other compounds, compound **7f** (IC_{50} = 5.6 μM), **7j** (IC_{50} = 4.5 μM) and **7k** (IC_{50} = 5.7 μM) have found to possess effective *E. coli* FabH inhibitory activity.

Structure Activity Relationship (SAR) was carried out from antibacterial and anticancer activities. According to the activity data, it has been observed that the change in R_1, R_2 and R_3 substitutions may lead to change in the activity against employed strains and cancer cells. In the case of both activities, R_1 = CH_3 and Cl may play an important role for the better activity, while R_1 = H may decrease the activity. Besides, in the case of antibacterial activity, R_2 = H is more effective than R_2 = CH_3 against Gram negative bacteria, while R_2 = H and R_3 = COOEt against Gram positive bacteria may play an important role for the better activity. Moreover, reviewing and comparing the activity data, it is worthy to mention that the antibacterial and anticancer activities of the target compounds depend not only on the bicyclic heteroaromatic pharmacophore, but also on the nature of the substituents.

Generally, in the molecular modeling, the most stable protein–ligand complex structure can be obtained by binding of compound into the active site of protein with lowest binding energy. Due this stability, particular compounds lead to the efficient activity. In the case of antibacterial activity, our modeling results revealed that the compound **7b** (R_1 = CH_3, R_2 = H, R_3 = CN) showed lowest binding energy by interaction with FabH leads to stable protein-ligand complex. The lowest binding energy may lead to the improvement in the activity, while increasing of the binding energy and poor activity was observed in compound **7d** (R_1 = H, R_2 = CH_3, R_3 = CN). In the case of anticancer activity, –CH_3 at R_1 and R_2 position, and –COOEt at R_3 position (**7k**) may responsible for most effective activity by binding into the active pocket of EGFR with lowest binding energy. This also creates the most stable protein–ligand complex structure than other compounds of the series. In brief, it has been observed that compounds having R_1 = CH_3 were found to have lower binding energies and efficient antibacterial as well as anticancer activity.

4.2.3. Molecular docking study with EGFR

To gain better understanding on the potency of all compounds and guide further SAR studies, we proceeded to examine the interaction of those with EGFR (PDB code: 1M17) by molecular docking, which was performed by simulation of compounds into the ATP binding site in EGFR. The binding energy of all the compounds is mentioned in Table 4. Of the compounds studied,

Table 4
Binding energy of compounds **7a**–**l** with EGFR.

Compounds	Binding energy ΔG_b
7a	−47.5404
7b	−44.2319
7c	−48.4589
7d	−38.3829
7e	−47.2833
7f	−43.7073
7g	−49.4853
7h	−52.0321
7i	−48.6366
7j	−47.0647
7k	**−54.6913**
7l	−51.9798

Bold number indicate the lower binding energy.

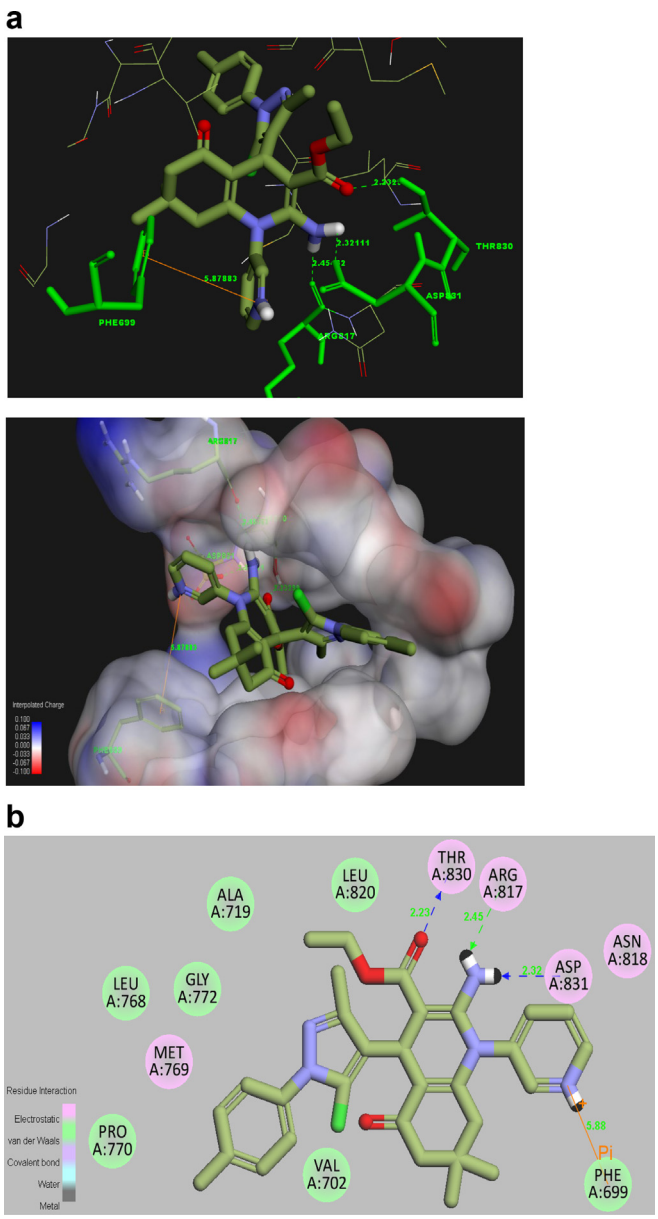

Fig. 1. (a) 3D binding model of compound **7k** into the active pocket of EGFR. (b) 2D binding model of compound **7k** into the active pocket of EGFR.

compound **7k** was nicely bound into the active site of EGFR with minimum binding energy ΔG_b = −54.6913 kcal/mol. The binding model of compound **7k** and EGFR was depicted in Fig. 1a and b. The amino acid residues which had interaction with EGFR were labeled. In the binding mode, compound **7k** was nicely bound to the ATP binding site of EGFR through hydrophobic interaction and the binding was stabilized by three hydrogen bonds and one π−cation interaction. Among them one hydrogen bond forms H atom of −NH2 group and ARG817 (distance: 2.45462 Å, DHA angle: 172.9°, HAY angle: 147.4°), second one between O atom of carbonyl group and THR830 (distance: 2.23299 Å, DHA angle: 138.3°, HAY angle: 139.3°), and third one between H atom of $-NH_2$ group and ASP831 (distance: 2.32111 Å, DHA angle: 103.1°, HAY angle: 163.8°). One π−cation bond forms between N atom of pyridine ring and PHE699 with distance 5.87883 Å. From this binding model, it could be concluded that three hydrogen bond and π−cation interaction are responsible for the effective EGFR inhibitory of compound **7k**.

4.2.4. Molecular docking study with FabH

Similarly, to gain better understanding on the potency of all compounds and guide further SAR studies, molecular docking of compounds and *E. coli* FabH was performed on the binding model based on the *E. coli* FabH−CoA complex structure (PDB code: 1HNJ). The FabH active site generally contains a catalytic triad tunnel consisting of Cys-His-Asn, which is conserved in various bacteria. This catalytic triad plays an important role in the regulation of chain elongation and substrate binding. Since the alkyl chain of CoA is broken by Cys of the catalytic triad of FabH, interactions between Cys and substrate appear to play an important role in substrate binding. Of the compounds studied, compound **7b** was nicely bound to active site of the FabH with hydrogen bonds and π−sigma interactions with minimum binding energy ΔG_b = −45.9125 kcal/mol. The binding energy of all the compounds is mentioned in Table 5. The binding model of compound **7b** and FabH was depicted in Fig. 2a and b. Among them hydrogen bonds formed with between oxygen atom of cyclohexanedione ring and ASN210 (distance: 2.37469 Å, DHA angle: 161.5°, HAY angle: 104.1°) and π−sigma interaction formed between pyrazole ring and GLY209 with distance: 2.63465 Å. From this binding model, it could be concluded that hydrogen and π−sigma interaction are responsible for the effective FabH inhibitory of compound **7b**.

5. Conclusion

In conclusion, the aim of the present investigation was to design a new series of 4*H*-quinoline derivatives by introduction

Table 5
Binding energy of compounds **7a**–**l** with FabH.

Compounds	Binding energy ΔG_b
7a	−38.9723
7b	**−45.9125**
7c	−37.9588
7d	−35.1931
7e	−38.3578
7f	−39.7733
7g	−37.8427
7h	−38.6283
7i	−39.8193
7j	−40.1617
7k	−39.7644
7l	−39.7296

Bold number indicate the lower binding energy.

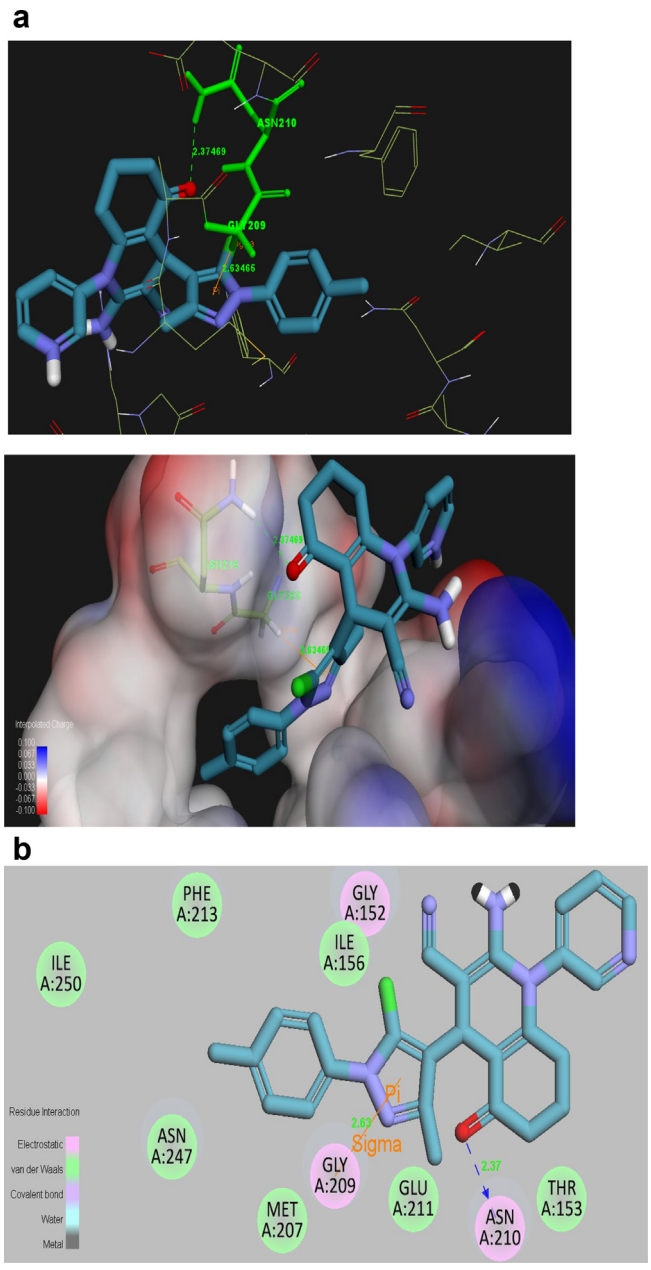

Fig. 2. (a) 3D binding model of compound **7b** into the active site of FabH. (b) 2D binding model of compound **7b** into the active site of FabH.

of substituted 1*H*-pyrazole at the C-4 position and pyridine ring at N-1 position for aiming their potent antimicrobial and anticancer activities. Some magnificent biological results have been obtained with the pyrazole–quinolone–pyridine hybridized scaffold and it has been concluded that majority of the compounds showed effective antibacterial as well as anticancer activities. In the case of inhibitory activity, compounds **7h**, **7k** and **7l** against EGFR as well as compounds **7b**, **7f**, **7j** and **7k** against FabH have found to be most effective members of the series. According to this, it is worthy to mention that the pyrazole–quinoline–pyridine hybrids as a useful template for further development of more antimicrobial and anticancer compounds that deserve further investigation and derivatization in order to discover the scope and limitation of its biological activities.

6. Experimental

6.1. Chemistry

All chemicals and reagents used in the current study were of analytical grade. Melting points (uncorrected) were determined on an XT4 MP apparatus (Taike Corp., Beijing, China). All the ^{1}H NMR and ^{13}C NMR spectra were recorded on a Bruker DPX300 model Spectrometer in DMSO-d_6 and chemical shifts were reported in ppm (d). FTIR spectra (KBr) were run on a Nexus 870 FT-IR spectrophotometer. ESI-MS spectra were recorded on a Mariner System 5304 mass spectrometer. Elemental analyses were performed on a CHN-O-Rapid instrument. TLC was performed on the glass backed silica gel sheets (Silica Gel 60 GF254) and visualized in UV light (254 nm).

6.1.1. General procedure for the synthesis of compounds *7a–l*

A 100 mL round bottomed flask, fitted with a reflux condenser, was charged with a mixture of 5-chloro-3-methyl-1-phenyl-1*H*-pyrazole-4-carbaldehyde **2a–c** (1 mmol), β-enaminone **5a**, **b** (1 mmol), malononitrile/ethylcyanoacetate **6a**, **b** (1 mmol) and a catalytic amount of piperidine (0.2 mmol) in ethanol (10 mL). The reaction mixture was heated under reflux for 2.5–3 h and the progress of the reaction was monitored by TLC. After the completion of reaction (as evidenced by TLC), the reaction mixture was cooled to room temperature and stirred magnetically for further 20 min, the solid mass separated was collected by filtration, washed well with ethanol (15 mL) and purified by leaching in equal volume ratio of chloroform and methanol (15 mL) to obtain pure solid sample **7a–l**.

*6.1.1.1. 2-Amino-4-(5-chloro-3-methyl-1-phenyl-1H-pyrazol-4-yl)-5-oxo-1-(pyridin-3-yl)-1,4,5,6,7,8-hexahydroquinoline-3-carbonitrile (**7a**).* Yield: 89%; mp 250–252 °C; IR (KBr, ν_{max}, cm^{-1}): 3435 & 3155 (asym. & sym. stretching of NH_2), 2195 (C≡N stretching), 1670 (C=O stretching), 750 (C–Cl stretching); ^{1}H NMR (DMSO-d_6) δ ppm: 1.66–2.24 (m, 6H, 3× CH_2), 2.41 (s, 3H, CH_3), 5.17 (s, 1H, quinoline H4), 5.60 (s, 2H, NH_2), 7.62–8.68 (m, 9H, Ar–H); ^{13}C NMR (DMSO-d_6) δ ppm: 12.98 (Ar–CH_3), 21.23, 28.73 (2C, CH_2), 34.60 (C4), 36.34 ($\underline{C}H_2$–CO), 59.58 ($\underline{C}$–CN), 112.19, 119.22, 121.80, 125.53, 127.44, 130.27, 132.12, 136.19, 138.23, 142.18, 144.17, 148.45, 150.20, 151.47, 153.59, 159.41 (16C, Ar–C), 195.54 (C=O); Anal. Calcd. for $C_{25}H_{21}ClN_6O$ (456.93 g/mol): C, 65.71; H, 4.63; N, 18.39 (%); Found: C, 65.48; H, 4.87; N, 18.17 (%). MS (*m*/*z*): 456.1 (M^+), 458.1 [M + 2].

*6.1.1.2. 2-Amino-4-(5-chloro-3-methyl-1-p-tolyl-1H-pyrazol-4-yl)-5-oxo-1-(pyridin-3-yl)-1,4,5,6,7,8-hexahydroquinoline-3-carbonitrile (**7b**).* Yield: 84%; mp 242–244 °C; IR (KBr, ν_{max}, cm^{-1}): 3430 & 3160 (asym. & sym. stretching of NH_2), 2185 (C≡N stretching), 1675 (C=O stretching), 760 (C–Cl stretching); ^{1}H NMR (DMSO-d_6) δ ppm: 1.72–2.32 (m, 6H, 3× CH_2), 2.36, 2.44 (s, 6H, 2× CH_3), 5.15 (s, 1H, quinoline H4), 5.59 (s, 2H, NH_2), 7.55–8.59 (m, 8H, Ar–H); ^{13}C NMR (DMSO-d_6) δ ppm: 12.90, 19.40 (Ar–CH_3), 21.28, 28.66 (2C, CH_2), 34.66 (C4), 36.30 ($\underline{C}H_2$–CO), 59.64 ($\underline{C}$–CN), 111.90, 120.17, 122.01, 125.45, 127.68, 130.88, 132.21, 136.11, 138.47, 142.36, 144.45, 148.98, 150.17, 151.40, 153.47, 159.69 (16C, Ar–C), 195.50 (C=O); Anal. Calcd. for $C_{26}H_{23}ClN_6O$ (470.95 g/mol): C, 66.31; H, 4.92; N, 17.84 (%); Found: C, 66.52; H, 5.13; N, 17.63 (%). MS (*m*/*z*): 470.2 (M^+), 472.2 [M + 2].

*6.1.1.3. 2-Amino-4-(5-chloro-1-(4-chlorophenyl)-3-methyl-1H-pyrazol-4-yl)-5-oxo-1-(pyridin-3-yl)-1,4,5,6,7,8-hexahydroquinoline-3-carbonitrile (**7c**).* Yield: 75%; mp 218–220 °C; IR (KBr, ν_{max}, cm^{-1}): 3440 & 3150 (asym. & sym. stretching of NH_2), 2200 (C≡N stretching), 1660 (C=O stretching), 745 (C–Cl stretching); ^{1}H NMR (DMSO-d_6) δ ppm: 1.69–2.21 (m, 6H, 3× CH_2), 2.50 (s, 3H, CH_3), 5.19

(s, 1H, quinoline H4), 5.67 (s, 2H, NH_2), 7.62–8.73 (m, 8H, Ar–H); ^{13}C NMR (DMSO-d_6) δ ppm: 13.09 (Ar–CH_3), 21.20, 28.75 (2C, CH_2), 34.58 (C4), 36.39 (CH_2–CO), 59.55 (C–CN), 112.32, 119.87, 121.91, 125.43, 127.65, 130.42, 132.17, 136.19, 138.47, 142.36, 144.58, 148.32, 150.21, 151.45, 154.54, 159.53 (16C, Ar–C), 195.47 (C=O); Anal. Calcd. for $C_{25}H_{20}Cl_2N_6O$ (491.37 g/mol): C, 61.11; H, 4.10; N, 17.10 (%); Found: C, 61.39; H, 4.32; N, 17.32 (%). MS (*m*/*z*): 490.1 (M^+), 492.1 [M + 2].

*6.1.1.4. 2-Amino-4-(5-chloro-3-methyl-1-phenyl-1H-pyrazol-4-yl)-7,7-dimethyl-5-oxo-1-(pyridin-3-yl)-1,4,5,6,7,8-hexahydroquinoline-3-carbonitrile (**7d**).* Yield: 87%; mp 267–269 °C; IR (KBr, ν_{max}, cm^{-1}): 3435 & 3155 (asym. & sym. stretching of NH_2), 2205 (C≡N stretching), 1680 (C=O stretching), 740 (C–Cl stretching); ^{1}H NMR (DMSO-d_6) δ ppm: 0.84, 1.00 (s, 6H, 2× CH_3), 1.85–2.72 (m, 4H, 2× CH_2), 2.46 (s, 3H, CH_3), 5.12 (s, 1H, quinoline H4), 5.63 (s, 2H, NH_2), 7.51–8.55 (m, 9H, Ar–H); ^{13}C NMR (DMSO-d_6) δ ppm: 13.14 (Ar–CH_3), 26.99, 28.25 (2C, CH_3), 32.05 ($C(CH_3)_2$), 34.65 (C4), 38.03 (CH_2), 49.88 (CH_2–CO), 59.52 (C–CN), 112.22, 119.34, 121.67, 125.73, 127.58, 130.45, 132.34, 136.37, 138.61, 142.45, 144.71, 148.80, 150.20, 151.47, 153.59, 159.60 (16C, Ar–C), 195.07 (C=O); Anal. Calcd. for $C_{27}H_{25}ClN_6O$ (484.98 g/mol): C, 66.87; H, 5.20; N, 17.33 (%); Found: C, 66.58; H, 4.94; N, 17.57 (%). MS (*m*/*z*): 484.1 (M^+), 486.1 [M + 2].

*6.1.1.5. 2-Amino-4-(5-chloro-3-methyl-1-p-tolyl-1H-pyrazol-4-yl)-7,7-dimethyl-5-oxo-1-(pyridin-3-yl)-1,4,5,6,7,8-hexahydroquinoline-3-carbonitrile (**7e**).* Yield: 79%; mp 229–231 °C; IR (KBr, ν_{max}, cm^{-1}): 3445 & 3160 (asym. & sym. stretching of NH_2), 2190 (C≡N stretching), 1675 (C=O stretching), 755 (C–Cl stretching); ^{1}H NMR (DMSO-d_6) δ ppm: 0.82, 0.98 (s, 6H, 2× CH_3), 1.86–2.77 (m, 4H, 2× CH_2), 2.35, 2.39 (s, 6H, 2× CH_3), 5.14 (s, 1H, quinoline H4), 5.64 (s, 2H, NH_2), 7.62–8.68 (m, 8H, Ar–H); ^{13}C NMR (DMSO-d_6) δ ppm: 13.20, 19.60 (Ar–CH_3), 27.05, 28.28 (2C, CH_3), 32.00 ($C(CH_3)_2$), 34.63 (C4), 37.95 (CH_2), 49.85 (CH_2–CO), 59.60 (C–CN), 111.89, 120.02, 122.15, 125.45, 127.64, 130.45, 132.17, 136.30, 138.64, 142.43, 144.70, 148.24, 119.15, 151.40, 154.15, 160.19 (16C, Ar–C), 194.99 (C=O); Anal. Calcd. for $C_{28}H_{27}ClN_6O$ (499.01 g/mol): C, 67.39; H, 5.45; N, 16.84 (%); Found: C, 67.54; H, 5.19; N, 17.05 (%). MS (*m*/*z*): 498.2 (M^+), 500.2 [M + 2].

*6.1.1.6. 2-Amino-4-(5-chloro-1-(4-chlorophenyl)-3-methyl-1H-pyrazol-4-yl)-7,7-dimethyl-5-oxo-1-(pyridin-3-yl)-1,4,5,6,7,8-hexahydroquinoline-3-carbonitrile (**7f**).* Yield: 76%; mp 257–259 °C; IR (KBr, ν_{max}, cm^{-1}): 3440 & 3165 (asym. & sym. stretching of NH_2), 2195 (C≡N stretching), 1665 (C=O stretching), 765 (C–Cl stretching); ^{1}H NMR (DMSO-d_6) δ ppm: 0.85, 1.01 (s, 6H, 2× CH_3), 1.88–2.75 (m, 4H, 2× CH_2), 2.40 (s, 3H, CH_3), 5.16 (s, 1H, quinoline H4), 5.69 (s, 2H, NH_2), 7.60–8.71 (m, 8H, Ar–H); ^{13}C NMR (DMSO-d_6) δ ppm: 13.05 (Ar–CH_3), 27.01, 28.20 (2C, CH_3), 32.03 ($C(CH_3)_2$), 34.61 (C4), 38.05 (CH_2), 50.00 (CH_2–CO), 59.62 (C–CN), 112.07, 119.84, 120.98, 125.28, 127.23, 130.40, 132.17, 136.30, 138.68, 142.46, 144.78, 148.80, 150.22, 151.40, 154.64, 160.10 (16C, Ar–C), 195.87 (C=O); Anal. Calcd. for $C_{27}H_{24}Cl_2N_6O$ (519.43 g/mol): C, 62.43; H, 4.66; N, 16.18 (%); Found: C, 62.72; H, 4.88; N, 15.91 (%). MS (*m*/*z*): 518.1 (M^+), 520.1 [M + 2].

*6.1.1.7. Ethyl 2-amino-4-(5-chloro-3-methyl-1-phenyl-1H-pyrazol-4-yl)-5-oxo-1-(pyridin-3-yl)-1,4,5,6,7,8-hexahydroquinoline-3-carboxylate (**7g**).* Yield: 88%; mp 276–278 °C; IR (KBr, ν_{max}, cm^{-1}): 3365 & 3180 (asym. & sym. stretching of NH_2), 1660 (C=O stretching), 1635 (C=O stretching), 760 (C–Cl stretching); ^{1}H NMR (DMSO-d_6) δ ppm: 0.97 (t, 3H, CH_3), 1.68–2.26 (m, 6H, 3× CH_2), 2.45 (s, 3H, CH_3), 3.93 (q, 2H, OCH_2), 5.30 (s, 1H, quinoline H4), 7.10 (s, 2H, NH_2), 7.54–8.70 (m, 9H, Ar–H); ^{13}C NMR (DMSO-d_6) δ ppm: 13.07 (Ar–CH_3), 14.73 (CH_3), 21.22, 28.70 (2C, CH_2), 36.42 (C4), 36.48 (CH_2–CO), 58.99 (OCH_2), 77.98 (C–COOEt), 112.24, 120.29, 125.31, 126.61, 127.12, 130.80, 139.79, 142.58, 145.76, 147.16, 151.52, 152.33, 152.47, 155.25, 159.69 (15C, Ar–C), 169.40 (COO), 195.49 (C=O); Anal. Calcd. for $C_{27}H_{26}ClN_5O_3$ (503.98 g/mol): C, 64.35; H, 5.20; N, 13.90 (%); Found: C, 64.62; H, 5.47; N, 14.15 (%). MS (*m*/*z*): 503.2 (M^+), 505.2 [M + 2].

*6.1.1.8. Ethyl 2-amino-4-(5-chloro-3-methyl-1-p-tolyl-1H-pyrazol-4-yl)-5-oxo-1-(pyridin-3-yl)-1,4,5,6,7,8-hexahydroquinoline-3-carboxylate (**7h**).* Yield: 83%; mp 235–237 °C; IR (KBr, ν_{max}, cm^{-1}): 3360 & 3175 (asym. & sym. stretching of NH_2), 1665 (C=O stretching), 1645 (C=O stretching), 750 (C–Cl stretching); ^{1}H NMR (DMSO-d_6) δ ppm: 0.95 (t, 3H, CH_3), 1.76–2.30 (m, 6H, 3× CH_2), 2.37, 2.43 (s, 6H, 2× CH_3), 3.96 (q, 2H, OCH_2), 5.29 (s, 1H, quinoline H4), 7.08 (s, 2H, NH_2), 7.57–8.69 (m, 8H, Ar–H); ^{13}C NMR (DMSO-d_6) δ ppm: 13.16, 19.47 (Ar–CH_3), 14.70 (CH_3), 21.18, 28.64 (2C, CH_2), 35.19 (C4), 36.48 (CH_2–CO), 59.00 (OCH_2), 78.02 (C–COOEt), 112.45, 119.39, 125.20, 126.55, 126.98, 130.35, 139.27, 142.19, 145.95, 147.18, 151.70, 152.17, 152.30, 155.11, 160.05 (15C, Ar–C), 169.48 (COO), 195.62 (C=O); Anal. Calcd. for $C_{28}H_{28}ClN_5O_3$ (518.01 g/mol): C, 64.92; H, 5.45; N, 13.52 (%); Found: C, 65.19; H, 5.29; N, 13.67 (%). MS (*m*/*z*): 517.2 (M^+), 519.2 [M + 2].

*6.1.1.9. Ethyl 2-amino-4-(5-chloro-1-(4-chlorophenyl)-3-methyl-1H-pyrazol-4-yl)-5-oxo-1-(pyridin-3-yl)-1,4,5,6,7,8-hexahydroquinoline-3-carboxylate (**7i**).* Yield: 71%; mp 272–274 °C; IR (KBr, ν_{max}, cm^{-1}): 3370 & 3190 (asym. & sym. stretching of NH_2), 1665 (C=O stretching), 1645 (C=O stretching), 755 (C–Cl stretching); ^{1}H NMR (DMSO-d_6) δ ppm: 0.98 (t, 3H, CH_3), 1.65–2.18 (m, 6H, 3× CH_2), 2.48 (s, 3H, CH_3), 3.94 (q, 2H, OCH_2), 5.38 (s, 1H, quinoline H4), 7.11 (s, 2H, NH_2), 7.61–8.76 (m, 8H, Ar–H); ^{13}C NMR (DMSO-d_6) δ ppm: 12.93 (Ar–CH_3), 14.74 (CH_3), 21.26, 28.72 (2C, CH_2), 35.22 (C4), 36.44 (CH_2–CO), 58.95 (OCH_2), 78.05 (C–COOEt), 112.48, 119.65, 125.63, 126.94, 127.20, 130.67, 139.82, 143.03, 146.13, 147.23, 151.80, 152.18, 152.40, 156.11, 159.11 (15C, Ar–C), 169.35 (COO), 195.57 (C=O); Anal. Calcd. for $C_{27}H_{25}Cl_2N_5O_3$ (538.43 g/mol): C, 60.23; H, 4.68; N, 13.01(%); Found: C, 60.01; H, 4.90; N, 13.26 (%). MS (*m*/*z*): 537.1 (M^+), 539.1 [M + 2].

*6.1.1.10. Ethyl 2-amino-4-(5-chloro-3-methyl-1-phenyl-1H-pyrazol-4-yl)-7,7-dimethyl-5-oxo-1-(pyridin-3-yl)-1,4,5,6,7,8-hexahydroquinoline-3-carboxylate (**7j**).* Yield: 82%; mp 223–225 °C; IR (KBr, ν_{max}, cm^{-1}): 3355 & 3185 (asym. & sym. stretching of NH_2), 1670 (C=O stretching), 1640 (C=O stretching), 760 (C–Cl stretching); ^{1}H NMR (DMSO-d_6) δ ppm: 0.83 (s, 3H, CH_3), 0.96 (t, 3H, CH_3), 0.99 (s, 3H, CH_3), 1.84–2.74 (m, 4H, 2× CH_2), 2.38 (s, 3H, CH_3), 3.95 (q, 2H, OCH_2), 5.25 (s, 1H, quinoline H4), 7.09 (s, 2H, NH_2), 7.53–8.68 (m, 9H, Ar–H); ^{13}C NMR (DMSO-d_6) δ ppm: 13.01 (Ar–CH_3), 14.79 (CH_3), 26.95, 28.19 (2C, CH_3), 32.02 ($C(CH_3)_2$), 34.23 (C4), 37.99 (CH_2), 49.90 (CH_2–CO), 59.03 (OCH_2), 78.00 (C–COOEt), 111.96, 119.28, 124.94, 126.73, 127.26, 131.12, 140.13, 143.17, 145.54, 147.09, 152.07, 152.38, 152.61, 155.96, 160.16 (15C, Ar–C), 169.32 (COO), 195.15 (C=O); Anal. Calcd. for $C_{29}H_{30}ClN_5O_3$ (532.03 g/mol): C, 65.47; H, 5.68; N, 13.16 (%); Found: C, 65.78; H, 5.96; N, 12.86 (%). MS (*m*/*z*): 531.2 (M^+), 533.2 [M + 2].

*6.1.1.11. Ethyl 2-amino-4-(5-chloro-3-methyl-1-p-tolyl-1H-pyrazol-4-yl)-7,7-dimethyl-5-oxo-1-(pyridin-3-yl)-1,4,5,6,7,8-hexahydroquinoline-3-carboxylate (**7k**).* Yield: 79%; mp 280–282 °C; IR (KBr, ν_{max}, cm^{-1}): 3350 & 3180 (asym. & sym. stretching of NH_2), 1675 (C=O stretching), 1635 (C=O stretching), 770 (C–Cl stretching); ^{1}H NMR (DMSO-d_6) δ ppm: 0.86 (s, 3H, CH_3), 0.97 (t, 3H, CH_3), 0.98 (s, 3H, CH_3), 1.88–2.73 (m, 4H, 2× CH_2), 2.36, 2.47 (s, 6H, 2× CH_3), 3.92 (q, 2H, OCH_2), 5.32 (s, 1H, quinoline H4), 7.13 (s, 2H, NH_2), 7.54–8.69 (m, 8H, Ar–H); ^{13}C NMR (DMSO-d_6) δ ppm:

13.04, 19.52 (Ar–CH_3), 14.77 (CH_3), 27.03, 28.17 (2C, CH_3), 32.09 ($\underline{C}(CH_3)_2$), 34.28 (C4), 38.10 (CH_2), 50.02 ($\underline{C}H_2$–CO), 58.97 (O$\underline{C}H_2$), 77.95 ($\underline{C}$–COOEt), 112.16, 119.58, 125.47, 126.78, 127.23, 130.45, 139.65, 143.14, 145.93, 148.20, 151.84, 151.98, 152.40, 155.17, 159.79 (15C, Ar–C), 169.44 ($\underline{C}$OO), 195.02 (C=O); Anal. Calcd. for $C_{30}H_{32}ClN_5O_3$ (546.06 g/mol): C, 65.99; H, 5.91; N, 12.83 (%); Found: C, 65.65; H, 6.14; N, 13.15 (%). MS (*m*/*z*): 545.2 (M^+), 547.2 [M + 2].

*6.1.1.12. Ethyl 2-amino-4-(5-chloro-1-(4-chlorophenyl)-3-methyl-1H-pyrazol-4-yl)-7,7-dimethyl-5-oxo-1-(pyridin-3-yl)-1,4,5,6,7,8-hexahydroquinoline-3-carboxylate (**7l**).* Yield: 73%; mp 262–264 °C; IR (KBr, ν_{max}, cm^{-1}): 3365 & 3185 (asym. & sym. stretching of NH_2), 1665 (C=O stretching), 1640 (C=O stretching), 765 (C–Cl stretching); ^{1}H NMR (DMSO-d_6) δ ppm: 0.84 (s, 3H, CH_3), 0.98 (t, 3H, CH_3), 0.99 (s, 3H, CH_3), 1.87–2.74 (m, 4H, 2× CH_2), 2.43 (s, 3H, CH_3), 3.94 (q, 2H, OCH_2), 5.28 (s, 1H, quinoline H4), 7.12 (s, 2H, NH_2), 7.63–8.74 (m, 8H, Ar–H); ^{13}C NMR (DMSO-d_6) δ ppm: 13.10 (Ar–CH_3), 14.72 (CH_3), 26.97, 28.23 (2C, CH_3), 32.01 ($\underline{C}(CH_3)_2$), 34.26 (C4), 37.93 (CH_2), 49.96 ($\underline{C}H_2$–CO), 58.93 (O$\underline{C}H_2$), 77.97 ($\underline{C}$–COOEt), 112.25, 120.20, 125.43, 126.72, 127.21, 131.04, 139.84, 142.60, 146.11, 147.22, 151.82, 152.19, 153.16, 156.01, 160.14 (15C, Ar–C), 169.38 ($\underline{C}$OO), 195.10 (C=O); Anal. Calcd. for $C_{29}H_{29}Cl_2N_5O_3$ (566.48 g/mol): C, 61.49; H, 5.16; N, 12.36 (%); Found: C, 61.74; H, 5.41; N, 12.73 (%). MS (*m*/*z*): 565.2 (M^+), 567.2 [M + 2].

Acknowledgment

This work was supported by the National Forestry Commonweal Project (200904001), by the project (No. BY2012136) from the Science & Technology Agency of Jiangsu Province and by the projects (Nos. CXY1213 & CXY1222) from the Science & Technology Bureau of Lianyuangang City of Jiangsu Province.

Appendix A. Supplementary data

Supplementary data related to this article can be found at http://dx.doi.org/10.1016/j.ejmech.2014.01.018.

References

[1] M. Gallorini, A. Cataldi, V. di Giacomo, Biodrugs 26 (2012) 377–391.
[2] J. Cicenas, M. Valius, J. Cancer Res. Clin. 137 (2011) 1409–1418.
[3] D.J. Slamon, G.M. Clark, S.G. Wong, W.J. Levin, A. Ullrich, W.L. McGuire, Science 235 (1987) 177–182.
[4] D.J. Slamon, W. Godolphin, L.A. Jones, Science (Washington DC) 244 (1989) 707–712.
[5] K.S. Kolibaba, B. Druker, J. Biochim. Biophys. Acta 1333 (1997) 217–248.
[6] M. Tateishi, T. Ishida, T. Mitsudomi, S. Kaneko, K. Sugimachi, Cancer Res. 50 (1990) 7077–7080.
[7] T.P. Fleming, A. Saxena, W.C. Clark, J.T. Robertson, E.H. Oldfield, S.A. Aaronson, I.U. Ali, Cancer Res. 52 (1992) 4550–4553.
[8] D.M. Shin, J.Y. Ro, W.K. Hong, W.N. Hittelamn, Cancer Res. 54 (1994) 3153–3159.
[9] F. Ciardiello, G. Tortola, Clin. Cancer Res. 7 (2001) 2958–2970.
[10] M. Leeb, Nature 431 (2004) 892–893.
[11] J.-Y. Lee, K.-W. Jeong, J.-U. Lee, D.-I. Kang, Y. Kim, Bioorg. Med. Chem. 17 (2009) 5408–5413.
[12] C.Y. Lai, J.E. Cronan, J. Biol. Chem. 19 (2003) 51494–51503.
[13] Y.J. Lu, Y.M. Zhang, C.O. Rock, Biochem. Cell. Biol. 82 (2004) 145–155.
[14] S.W. White, J. Zheng, Y.M. Zhang, C.O. Rock, Annu. Rev. Biochem. 74 (2005) 791–831.
[15] A. Asheka, S.J. Cho, Bioorg. Med. Chem. 14 (2006) 1474–1482.
[16] C.B. Sangani, D.C. Mungra, M.P. Patel, R.G. Patel, Cent. Eur. J. Chem. 9 (2011) 635–647.
[17] H.H. Jardosh, C.B. Sangani, M.P. Patel, R.G. Patel, Chin. Chem. Lett. 24 (2013) 123–126.
[18] C.B. Sangani, D.C. Mungra, M.P. Patel, R.G. Patel, Chin. Chem. Lett. 23 (2012) 57–60.
[19] C.B. Sangani, N.M. Shah, M.P. Patel, R.G. Patel, J. Serb. Chem. Soc. 77 (2012) 1165–1174.
[20] N.J. Thumar, M.P. Patel, J. Heterocycl. Chem. 49 (2012) 1169–1178.
[21] N.J. Thumar, M.P. Patel, Arch. Pharm. Chem. Life Sci. 334 (2011) 91–101.
[22] M.A. Gouda, M.A. Berghot, A.I. Shoeib, A.M. Khalil, Eur. J. Med. Chem. 45 (2010) 1843–1848.
[23] A.A. Bekhit, H.M.A. Ashour, Y.S.A. Ghany, A.E.A. Bekhit, A.M. Baraka, Eur. J. Med. Chem. 43 (2008) 456–463.
[24] P.T. Chovatia, J.D. Akabari, P.K. Kachhadia, P.D. Zalawadia, H.S. Joshi, J. Serb. Chem. Soc. 71 (2007) 713–720.
[25] H.T.Y. Fahmy, S.A.F. Rostom, A.A. Bekhit, Arch. Pharm. Chem. Life Sci. 335 (2002) 213–222.
[26] A.H. Abadi, A.A.H. Eissa, G.S. Hassan, Chem. Pharm. Bull. 51 (2003) 838–844.
[27] H.A. Abdel-Aziz, H.S.A. El-Zahabi, K.M. Dawood, Eur. J. Med. Chem. 45 (2010) 2427–2432.
[28] Y.-R. Liu, J.-Z. Luo, P.-P. Duan, J. Shao, B.-X. Zhao, J.-Y. Miao, Bioorg. Med. Chem. Lett. 22 (2012) 6882–6887.
[29] I. Vujasinovic, A. Paravic-Radicevic, K. Mlinaric-Majerski, K. Brajsa, B. Bertosa, Bioorg. Med. Chem. 20 (2012) 2101–2110.
[30] A.M. Farag, K.A.K. Ali, T.M.A. El-Debss, A.S. Mayhoub, A.E. Amr, N.A. Abdel-Hafez, M.M. Abdulla, Eur. J. Med. Chem. 45 (2010) 5887–5898.
[31] P. Lv, J. Sun, Y. Luo, Y. Yang, H.-L. Zhu, Bioorg. Med. Chem. Lett. 20 (2010) 4657–4660.
[32] H.H. Jardosh, M.P. Patel, Eur. J. Med. Chem. 65 (2013) 348–359.
[33] K.D. Thomas, A.V. Adhikari, S. Telkar, I.H. Chowdhury, R. Mahmoode, N.K. Pal, G. Rowd, E. Sumesh, Eur. J. Med. Chem. 46 (2011) 5283–5292.
[34] K. Starcevic, D. Pesic, A. Toplak, G. Landek, S. Alihodzic, E. Herreros, S. Ferrer, R. Spaventi, M. Peric, Eur. J. Med. Chem. 49 (2012) 365–378.
[35] P.A. Leatham, H.A. Bird, V. Wright, D. Seymour, A. Gordon, Eur. J. Rheumatol. Inflamm. 6 (1983) 209–211.
[36] H.G. Kathrotiya, M.P. Patel, Eur. J. Med. Chem. 63 (2013) 675–684.
[37] N. Muruganantham, R. Sivakumar, N. Anbalagan, V. Gunasekaran, J.T. Leonard, Biol. Pharm. Bull. 27 (2004) 1683–1687.
[38] M.P. Maguire, K.R. Sheets, K. McVety, A.P. Spada, A. Zilberstein, J. Med. Chem. 37 (1994) 2129–2137.
[39] A. Zieba, A. Sochanik, A. Szurko, M. Rams, A. Mrozek, P. Cmoch, Eur. J. Med. Chem. 45 (2010) 4733–4739.
[40] M. Gopal, S. Shenoy, L.S. Doddamani, J. Photochem. Photobiol. B 72 (2003) 69–78.
[41] Y.H. Kim, K.J. Shin, T.G. Lee, E. Kim, M.S. Lee, S.H. Ryu, Biochem. Pharmacol. 69 (2005) 1333–1341.
[42] Y.L. Zhao, Y.L. Chen, F.S. Chang, C.C. Tzeng, Eur. J. Med. Chem. 40 (2005) 792–797.
[43] M. Pannala, S. Kher, N. Wilson, J. Gaudette, L. Sircar, S. Zhang, A. Bakhirev, G. Yang, P. Yuen, F. Gorcsan, N. Sakurai, M. Barbosa, J. Cheng, Bioorg. Med. Chem. Lett. 17 (2007) 5978–5982.
[44] S. Prachayasittikul, L. Treeratanapiboon, S. Ruchirawat, V. Prachayasittikul, Excli J. 8 (2009) 121–129.
[45] E. Nassar, J. Am. Sci. 6 (2010) 338–343.
[46] Y. Maoa, W. Zhu, X. Kong, Z. Wang, H. Xie, J. Ding, N.K. Terrett, J. Shen, Bioorg. Med. Chem. 21 (2013) 3090–3104.
[47] J. Sinkkonen, V. Ovcharenko, K.N. Zelenin, I.P. Bezhan, B.A. Chakchir, F. Al-Assar, K. Pihlaja, Eur. J. Org. Chem. 13 (2002) 2046–2053.
[48] R.P. Jain, J.C. Vederas, Bioorg. Med. Chem. Lett. 14 (2004) 3655–3658.
[49] A. Kumar, M.K. Gupta, M. Kumar, Green Chem. 14 (2012) 290–295.
[50] H.-R. Tsou, N. Mamuya, B.D. Johnson, M.F. Reich, B.C. Gruber, F. Ye, R. Nilakantan, R. Shen, C. Discafani, R. DeBlanc, R. Davis, F.E. Koehn, L.M. Greenberger, Y.-F. Wang, A. .Wissner, J. Med. Chem. 41 (2001) 2719–2734.
[51] J. Meletiadis, J.F. Meis, J.W. Mouton, J.P. Donnelly, P.E. .Verweij, J. Clin. Microbiol. 38 (2000) 2949–2954.
[52] R. Huey, G.M. Morris, A.J. Olson, D.S. Goodsell, J. Comput. Chem. 28 (2007) 1145–1152.